Arabian Journal of Chemistry (2016) 9, 62–71

King Saud University

Arabian Journal of Chemistry

www.ksu.edu.sa
www.sciencedirect.com

ORIGINAL ARTICLE

Numerical simulation of CO_2 separation from gas mixtures in membrane modules: Effect of chemical absorbent

Seyed Mohammad Reza Razavi [a], Saeed Shirazian [a,*], Mahboobeh Nazemian [b]

[a] Young Researchers and Elite Club, South Tehran Branch, Islamic Azad University, Tehran, Iran
[b] Iran Polymer and Petrochemical Institute, Tehran, Iran

Received 3 April 2015; accepted 3 June 2015
Available online 18 June 2015

KEYWORDS

Separation;
Membrane;
Mathematical modeling;
Numerical simulation;
Mass transfer

Abstract In this study, a mathematical model is proposed for prediction of CO_2 absorption from N_2/CO_2 mixture by potassium threonate in a hollow-fiber membrane contactor (HFMC). CFD technique using numerical method of finite element was applied to solve the governing equations of model. Effect of different factors on CO_2 absorption was analyzed and for investigation of absorbent type effect, functioning of potassium threonate was compared with diethanolamine (DEA). Axial and radial diffusion can be described with the two dimensional model established in this work. The obtained simulation results were compared with the reported experimental data to ensure accuracy of the model predictions. Comparison of model results with experimental data revealed that the developed model can well predict CO_2 capture by potassium threonate in HFMCs. Increment of absorbent flow rate and concentration eventuate in enhancement of CO_2 absorption. On the other hand, capture of CO_2 will be reduced with increment of gas flow rate. According to the model results, potassium threonate can be considered as a more efficient absorbent as compared with DEA.

1. Introduction

CO_2 that normally exists in natural gas streams, biogas produced from anaerobic absorption, flue gas generated by combustion of fossil fuels, and coal gasification is the most important greenhouse gas on the earth (Zhang et al., 2013). CO_2 capture will improve the calorific value of natural gas (NG), reduce the volume of gas that is transported through the pipeline, decrease equipment corrosion and inhibit atmospheric pollution and global warming (Zhang et al., 2013; Chew et al., 2010; Razavi et al., 2015). Consequently there is a need to design a novel method to eliminate CO_2 from gas streams.

CO_2 can be removed from gas streams by different methods that two most important of them are absorption and membrane separation (Razavi et al., 2013; Fasihi et al., 2012;

* Corresponding author. Tel.: +98 9378459498.
E-mail address: saeed.shirazian@gmail.com (S. Shirazian).
Peer review under responsibility of King Saud University.

ELSEVIER Production and hosting by Elsevier

http://dx.doi.org/10.1016/j.arabjc.2015.06.006
1878-5352

Nomenclature

C	concentration (mol/m^3)
C_{outlet}	outlet concentration of solution the tube side (mol/m^3)
C_{inlet}	inlet concentration of solution the tube side (mol/m^3)
$C_{i\text{-}tube}$	concentration of solution the tube side (mol/m^3)
$C_{i\text{-}shell}$	concentration of solution the shell side (mol/m^3)
$C_{i\text{-}membrane}$	concentration of solution membrane (mol/m^3)
D	diffusion coefficient (m^2/s)
F	liquid feed flow (m^3/s)
m	physical solubility
P	pressure (pa)
r	radial coordinate (m)
r_1	inner tube radius (m)
r_2	outer tube radius (m)
r_3	inner shell radius (m)
u	average velocity in tube side (m/s)
z	axial coordinate
$V_{z\text{-shell}}$	z – velocity in the shell (m/s)
$V_{z\text{-tube}}$	z – velocity in the tube (m/s)

Shirazian et al., 2012a,b; Rezakazemi et al., 2013a; Ghadiri et al., 2013a; Shirazian and Ashrafizadeh, 2013, 2011; Fadaei et al., 2011). From the mentioned methods, absorption has been established as a well-accepted method at industrial applications (Adewole et al., 2013). However this method has some drawbacks such as expensive chemical solvents, low efficiency of process, production of large amounts of wastewater and sludge in the process, costly equipment, consumption of energy for solvent regeneration, high complexity of the processes, and negative environmental impact due to consumption of solvents (Thiruvenkatachari et al., 2009). Accordingly, there is a need to find an alternative technology that would be cost effective and energy efficient such as membrane separation for CO_2 removal from gas streams.

Nowadays, capture of CO_2 from gas streams using membrane separation technology has become an attractive approach as compared to the aforementioned separation methods (Yeo et al., 2012; Fadaei et al., 2011; Ghadiri and Shirazian, 2013). This method is more capital efficient and could achieve higher efficiency of separation with this method. Additionally, simplicity of process in modern compact modules, high reliability, low capital and operating cost of process, the nature of environmentally friendly, high space efficiency, low energy consumption, clean and continuous process are some of the advantages of application of membrane for gas separation which makes it favorable for large scale applications (Adewole et al., 2013; Yeo et al., 2012; Rezakazemi et al., 2013b; Ghadiri et al., 2013b).

As compared to different types of membranes, polymeric membranes that have low molecular weight, process ability into thin films, absorbent materials, composites and hollow fibers and large variety in structure and properties have the most usage in industrial applications (Zhang et al., 2013; Razavi et al., 2015; Yeo et al., 2012; Miramini et al., 2013). Numerous polymers that so far have been utilized for membranes fabrication used in gas separation, include cellulose acetate (CA), polyimide (PI), polysulfone (PSf), polyethersulfone (PES), and polycarbonates (PC) Zhang et al., 2013. Depending on different gas separation requirements, specific polymeric membrane is chosen and applied. Polysulfone and cellulose acetate are the earliest commercial membranes, while PI and CA have been mostly used for CO_2/CH_4 separation commercially (Han and Lee, 2011; Spillman, 1995).

Among the various kinds of membranes, hollow-fiber membrane contactors are the most desirable device since they present higher surface/volume ratio. In recent years, many researchers have focused on investigation of different factors affecting HFMCs performance such as different absorbents, various polymers as a membrane, and flow rate of gas and liquid (Fasihi et al., 2012; Ghadiri et al., 2013a,b,c, 2014a,b, 2015; Fadaei et al., 2011a,b, 2012; Miramini et al., 2013; Ghadiri and Ashrafizadeh, 2014; Marjani et al., 2012a,b, 2011a,b; Marjani and Shirazian, 2010, 2011a,b,c,d,e, 2012a).

In membrane gas absorption, the absorbent plays a vital role for CO_2 capture. Among the various absorbents, alkanolamines such as AMP, DEA, TEA, DGA, MEA, MEDA and DIPA have the most appliances as absorbent for removal of CO_2 from gas streams. Choosing a liquid absorbent depends on the properties of absorbent such as rate of reaction with CO_2, thermal stability, vapor pressure and easily regeneration (Razavi et al., 2013; Li and Chen, 2005; Blauwhoff et al., 1984).

Lu et al. studied effect of AMP and Piperazine as activators for solution of MDEA on CO_2 capture from gas mixture (Lu et al., 2007). Ren et al. investigated CO_2 capture by PVDF membranes and also the effect of process parameters on separation efficiency (Ren et al., 2006). With the aim of simulation, use of membrane separation for elimination of CO_2 from gas mixtures in industrial scale would become more easily and more cost effective. Simulations of HFMCs have attracted many research attentions. Mathematical modeling and numerical simulation of membrane contactors considering chemical reaction have been studied in the literature (Fasihi et al., 2012; Shirazian et al., 2012a,b; Shirazian and Ashrafizadeh, 2013, 2011; Fadaei et al., 2011a,b, 2012; Ghadiri and Shirazian, 2013; Ghadiri et al., 2013b,c, 2014a,b; Marjani et al., 2012a,b, 2011a,b; Marjani and Shirazian, 2010, 2011a,b,c,d,e, 2012a; Fazaeli et al., 2015; Tahvildari et al., 2016). The main aim of the simulation works was to determine the concentration of CO_2 in the membrane contactor. However, some works accounted for chemical reaction.

Although amine solutions have more uses in membrane gas separation as compared with other absorbents, they have some disadvantages including easily degradation, particularly in oxygenated atmosphere, corrosion and high volatility (Mandal and Bandyopadhyay, 2005; Portugal et al., 2008). Because of these disadvantages, researchers try to develop more suitable absorbents such as amino acid salt solutions. Stability of amino acid salt solutions in the oxygenated atmosphere is higher than alkanolamines. Because amino acid salt

solutions have ionic nature, not only they are less volatile but also they have high surface tensions. Potassium threonate is an amino acid salt that has a reasonable capacity in membrane separation of CO_2. Potassium threonate, in spite of good capability of regeneration, high surface tension and low volatility, is not deleterious for health (Portugal et al., 2008).

Portugal et al. (2008) investigated CO_2 capture in aqueous solution of Potassium threonate and determined densities and viscosities of aqueous solution at concentration range of 0.1–3 M and temperatures from 293 to 313 K. Their results showed that the pseudo-first-order reaction can be used to describe CO_2 absorption in the aqueous solution of Potassium threonate. Moreover, it was indicated that CO_2 absorption rate was enhanced by increasing CO_2 and potassium threonate concentrations (Portugal et al., 2008).

In this work, because of potassium threonate advantages along with advantages of membrane separation, capture of CO_2 by potassium threonate in HFMC is simulated. In addition to the investigation of influence of various parameters on CO_2 removal, performance of potassium threonate is compared with DEA for selecting the most effective one.

2. Mass transfer model

In the present work, a comprehensive 2D phenomenological model is developed for the capture of CO_2 from CO_2/N_2 gas stream in a hollow-fiber membrane contactor. Fig. 1 represents the schematic diagram of the HFMC simulated in this study. The membrane module consists of 21 fibers with an inner and outer diameter of 1.4 mm and 2.2 mm respectively within a module which has an outer diameter of 16 mm. Razavi et al. have provided a table containing geometrical characteristics of the simulated HFMC in their study (see Table 1) (Razavi et al., 2013). Gas mixture and liquid solution of chemical absorbent flow counter currently into the tube and shell of the HFMC respectively. Flow rate of gas mixture is kept between 100 and 400 cm^3/min and flow rate of liquid solution of absorbent is in the range of 50–350 cm^3/min. Absorbent concentration in liquid solution is 0.5 M.

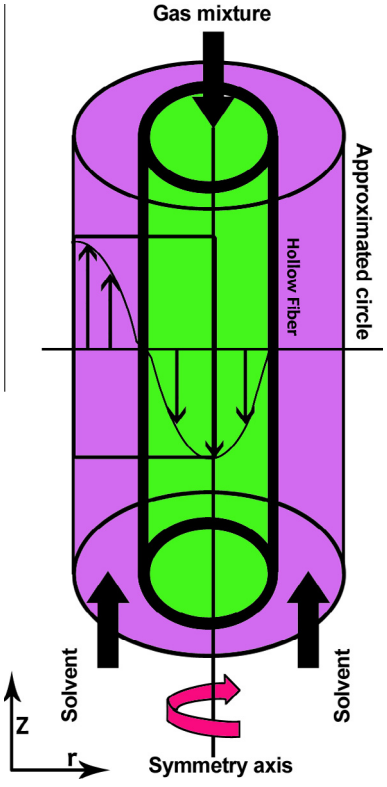

Figure 1 A graphical diagram for the hollow-fiber membrane contactor.

Table 1 Characteristics of hollow fiber module.

Module o.d. (mm)	16
Shell i.d. (mm)	14
Fiber o.d. (mm)	2.2
Fiber i.d. (mm)	1.4
Fiber length (cm)	31.4
Number of fibers	21
Average pore size (mm)	0.2
Fiber porosity, ε (%)	50
Surface area (m^2)	0.02

2.1. Model equation

By applying Navier–Stokes equation, velocity distribution in the tube side can be derived, but for developing velocity profile in the tube side, a fully developed Newtonian laminar flow is assumed (Bird et al., 1960):

$$V_{z\text{-}tube} = 2u\left[1 - \left(\frac{r}{r_1}\right)^2\right] \tag{1}$$

where r_1 and u indicate inner radius of fiber and average velocity of stream in the tube, respectively.

It should be noted that according to the free surface model, cross sectional area of fiber is considered to be circle-shaped (Happel, 1959). The continuity equation for each component can be expressed as follows (Bird et al., 1960):

$$\frac{\partial C_i}{\partial t} = -(\nabla \cdot C_i V) - (\nabla \cdot J_i) + R_i \tag{2}$$

where C_i, t, V, J_i and R_i indicate concentration (mol cm^{-3}), time (s), velocity (m/s), diffusion flux (mol m^{-2} s^{-1}) and reaction rate of component i (mol m^{-3} s^{-1}), respectively.

For simplifying Eq. (2), the process assumed to be steady state and J_i was substituted with Fick's law.

2.1.1. Tube side equations

In the tube side of HFMC there is no chemical reaction, addition to the fact that convective mass transfer in radial direction is not considerable in comparison with axial direction. Consequently Eq. (2) can be written as follows:

$$D_{CO_2\text{-}tube}\left[\frac{\partial^2 C_{CO_2\text{-}tube}}{\partial r^2} + \frac{1}{r}\frac{\partial C_{CO_2\text{-}tube}}{\partial r} + \frac{\partial^2 C_{CO_2\text{-}tube}}{\partial z^2}\right] = V_{z\text{-}tube}\frac{\partial C_{CO_2}}{\partial z} \tag{3}$$

where r and z denote the radial and axial coordinates, respectively.

Boundary conditions considered for the tube side are as follows:

$$\text{At } r = r_1,\ C_{CO_2\text{-}tube} = C_{CO_2\text{-}membrane} \tag{4}$$

$$\text{At } r = 0,\ \frac{\partial C_{CO_2\text{-}tube}}{\partial r} = 0 \tag{5}$$

$$\text{At } z = 0,\ \text{convective flux} \tag{6}$$

$$\text{At } z = L,\ C_{CO_2\text{-}tube} = C_{CO_2,0} \tag{7}$$

It should be noted that convective flux in Eq. (6) indicates that the mass transfer through this boundary by diffusion mechanism is neglected.

2.1.2. Shell side equations

The steady-state continuity equation in the shell side is expressed as follows:

$$D_{CO_2\text{-}Shell}\left[\frac{\partial^2 C_{CO_2\text{-}Shell}}{\partial r^2} + \frac{1}{r}\frac{\partial C_{CO_2\text{-}Shell}}{\partial r} + \frac{\partial^2 C_{CO_2\text{-}Shell}}{\partial z^2}\right] = V_{z\text{-}Shell}\frac{\partial C_{CO_2\text{-}Shell}}{\partial z} - R_{CO_2} \tag{8}$$

As stated before, by solving Navier–Stokes equation, velocity distribution in the shell side can be obtained (Bird et al., 1960) as follows:

$$-\nabla\cdot\eta(\nabla V_{z\text{-}Shell} + (\nabla V_{z\text{-}Shell})^T) + \rho(V_{z\text{-}Shell}\cdot\nabla)V_{z\text{-}Shell} + \nabla p$$
$$\nabla\cdot V_{z\text{-}Shell} = 0 \tag{9}$$

V (m/s), P (Pa), ρ (kg m^{-3}), η (kg m^{-1} s^{-1}) and F (N) denote velocity, pressure, density, dynamic viscosity and body force, respectively. The shell radius can be estimated by applying Happel free surface model as follows:

$$r_3 = \left(\frac{1}{1-\phi}\right)^{1/2} r_2 \tag{10}$$

where r_2 indicates the tube outer radius. Φ is the volume fraction of void section and can be defined by

$$1 - \phi = \frac{n r_2^2}{\Re^2} \tag{11}$$

where n and R are the number of fibers and inner radius of modules, respectively.

Boundary conditions used for the shell are as follows:

$$\text{At } r = r_3,\ \frac{\partial C_{CO_2\text{-}shell}}{\partial r} = 0 \tag{12}$$

$$\text{At } r = r_2,\ C_{CO_2\text{-}shell} = C_{CO_2\text{-}membrane} \times m \tag{13}$$

$$\text{At } z = 0,\ C_{CO_2\text{-}shell} = 0,\ V_{z\text{-}shell} = V_0 \tag{14}$$

$$\text{At } z = L,\ \text{Convective flux},\ p = p_{\text{atm}} \tag{15}$$

where m denotes solubility of CO_2 in absorber.

2.1.3. Membrane equations

Transport of CO_2 into the membrane pores is accomplished just via diffusion mechanism. Steady state and no reaction assumptions will simplify the continuity equation as follows:

$$D_{CO_2\text{-}membrane}\left[\frac{\partial^2 C_{CO_2\text{-}membrane}}{\partial r^2} + \frac{1}{r}\frac{\partial C_{CO_2\text{-}membrane}}{\partial r} + \frac{\partial^2 C_{CO_2\text{-}membrane}}{\partial z^2}\right] = 0 \tag{16}$$

In which boundary conditions can be written as follows:

$$\text{At } r = r_1,\ C_{CO_2\text{-}membrane} = C_{CO_2\text{-}shell} \tag{17}$$

$$\text{At } r = r_2,\ C_{CO2\text{-}membrane} = \frac{C_{CO_2\text{-}shell}}{m} \tag{18}$$

2.1.4. Absorbent equations

The steady state continuity equation for potassium threonate absorber is written as follows:

$$D_{i\text{-}shell}\left[\frac{\partial^2 C_{i\text{-}shell}}{\partial r^2} + \frac{1}{r}\frac{\partial C_{i\text{-}shell}}{\partial r} + \frac{\partial^2 C_{i\text{-}shell}}{\partial z^2}\right] = V_{z\text{-}shell}\frac{\partial C_{i\text{-}shell}}{\partial z} - R_i \tag{19}$$

R_i denotes the chemical reaction between CO_2 and potassium threonate absorbent (Portugal et al., 2008). Boundary conditions required for solving Eq. (19) are given as follows:

$$\text{At } r = r_3,\ \frac{\partial C_{absorbent\text{-}shell}}{\partial r} = 0 \tag{20}$$

$$\text{At } r = r_2,\ \frac{\partial C_{absorbent\text{-}shell}}{\partial r} = 0 \tag{21}$$

$$\text{At } z = 0,\ C_{\text{absorbent-shell}} = C_{\text{absorbent},0} \tag{22}$$

$$\text{At } z = L,\ \text{Convective flux} \tag{23}$$

2.2. Numerical procedure

The governing equations in membrane, tube and shell side were solved by the commercial finite element package of COMSOL Multiphysics version 3.5., according to the finite element method (FEM). Moreover solver of UMFPACK was used for solving symmetric problems. Some researchers have asserted the applicability and accuracy of UMFPACK for solving membrane equations (Razavi et al., 2013, 2014; Fasihi et al., 2012; Shirazian et al., 2012a,b,c,d,e; Rezakazemi et al., 2013a,b,c, 2011a,b, 2012; Shirazian and Ashrafizadeh, 2013, 2011, 2010a,b, 2014, 2015a,b,c; Fadaei et al., 2011a,b, 2012; Ghadiri et al., 2013b; Marjani et al., 2012a,b,c, 2011a,b; Marjani and Shirazian, 2010, 2011a,b,c,d,e, 2012a,b,c,d,e; Hemmati et al., 2015; Hoshyargar et al., 2012; Khansary et al., 2015; Kohnehshahri et al., 2011; Moghadassi et al., 2011; Mohammadi et al., 2015; Moradi et al., 2013; Nosratinia et al., 2015; Pishnamazi et al., 2012; Ranjbar et al., 2013; Shirazian et al., 2011a,b, 2009, 2014; Sohrabi et al., 2011a,b,c,d,e; Valavi et al., 2013). Triangular mesh elements used for the evaluation of gas behavior in the HFMC are illustrated in Fig. 2 in which r_1 and r_2 represent the radius of shell side and free surface respectively.

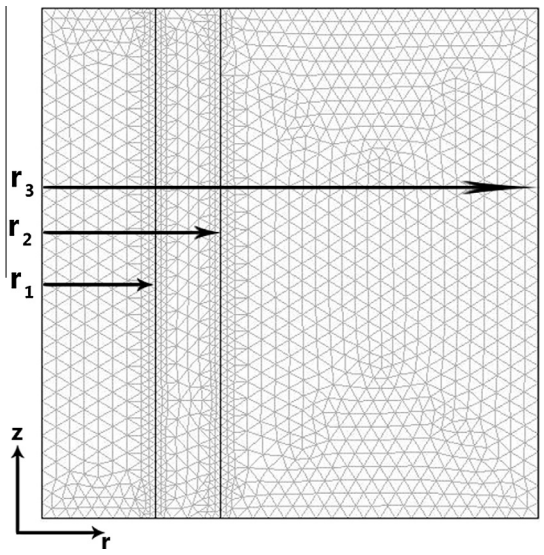

Figure 2 Model domain and FE model used for simulation.

3. Results and discussion

3.1. Model validation

According to author's investigations, absorption of CO_2 by potassium threonate using hollow-fiber membrane contactors has not been studied experimentally. Therefore, developed model in this study was validated through comparison of simulation results with experimental results of CO_2 removal from N_2 in the HFMC reported in the literature (Lin et al., 2008). As it can be seen in Fig. 3, there is a reasonable agreement between simulation results and experimental data. However, some deviations can be observed between experimental and modeling data which could be attributed to the estimation of reaction kinetics and constants.

3.2. Velocity distribution

Figs. 4 and 5 illustrate velocity distribution of absorbent inside the shell side of HFMC. It is clearly seen that the velocity profile is almost parabolic and reveals the maximum velocity of absorbent phase at the center of shell side. The latter could be due to the boundary conditions imposed on two sides of shell side and also the effects of viscous forces on the fluid which makes a symmetry velocity profile. Additionally,

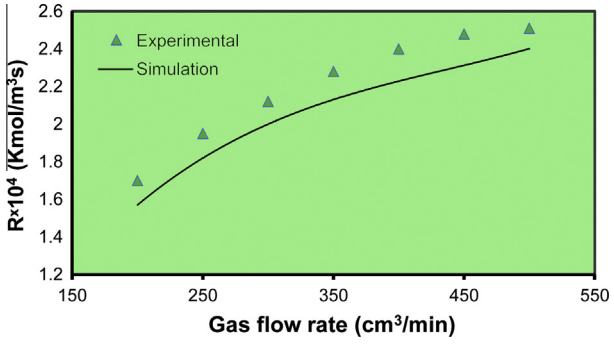

Figure 3 Relation between reaction rate and gas flow rates (for validation of model).

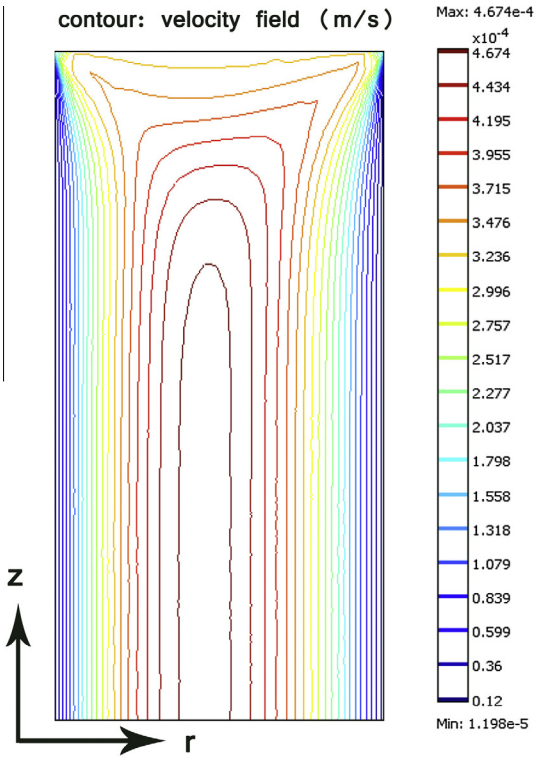

Figure 4 Velocity field in the shell side (absorbent channel) of the hollow-fiber membrane contactor.

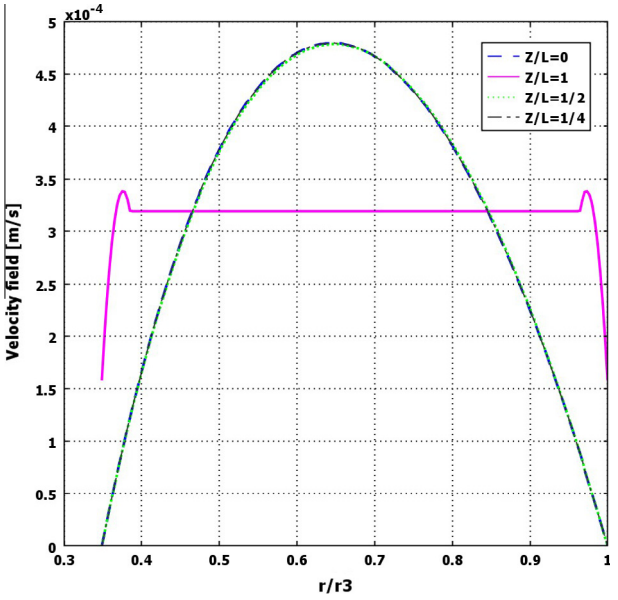

Figure 5 Velocity profile in the shell side (absorbent channel) along the membrane length.

velocity amount on the two shell walls is zero because of no-slip conditions. Figs. 4 and 5 also represent that after a short distance from entrance of shell side, velocity profile becomes fully developed. The velocity profile in Fig. 5 is depicted against dimensionless radial distance (r/r_3).

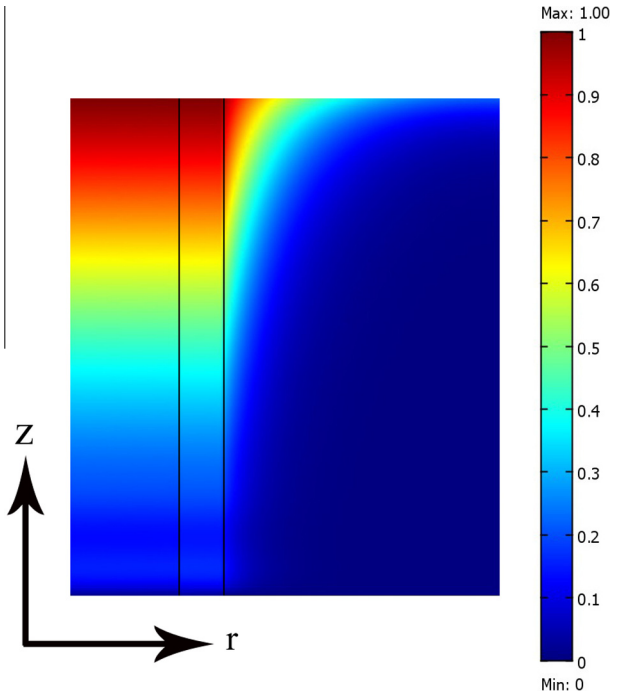

Figure 6 Dimensionless concentration distribution for CO_2 in the tube, the membrane and the shell of the HFMC.

3.3. Concentration distribution of CO_2

Distribution of dimensionless concentration (C/C_o) for CO_2 in the membrane, tube and shell side of the HFMC is illustrated in Fig. 6. While gas mixture flows from one side of the HFMC, in which CO_2 concentration is maximum, the potassium threonate solution flows from the other side in which gas concentration of CO_2 is considered to be zero. As the gas mixture flows through the tube, concentration difference caused CO_2 transferred to the membrane (Shirazian et al., 2012a; Ghadiri et al., 2013c; Shirazian and Ashrafizadeh, 2010a; Sohrabi et al., 2011c). Generally, the gas in the membrane contactor is transferred by two mechanisms, i.e. diffusion and convection. Diffusion is observed in radial direction due to concentration gradient, while convection is observed in axial direction due to velocity of fluid. However, in the tube side the diffusional mass transfer is favorable because it can increase the amount of CO_2 capture. Gas mixture is transferred through the membrane pores to the other side and the moving solvent in the shell side could absorb the CO_2.

Fig. 7 illustrates the distribution of CO_2 concentration in the tube in the axial direction. CO_2 concentration reduces with increasing the length of membrane due to CO_2 removal by absorbent solution. Additionally, variation rate of CO_2 along the HFMC has not been altered significantly.

3.4. Concentration distribution of the absorbent

Fig. 8 shows a representation of the distribution of dimensionless concentration of potassium threonate in the shell side of HFMC. When CO_2 diffuses through the membrane pores, it reacts with potassium threonate solution flowing in the shell

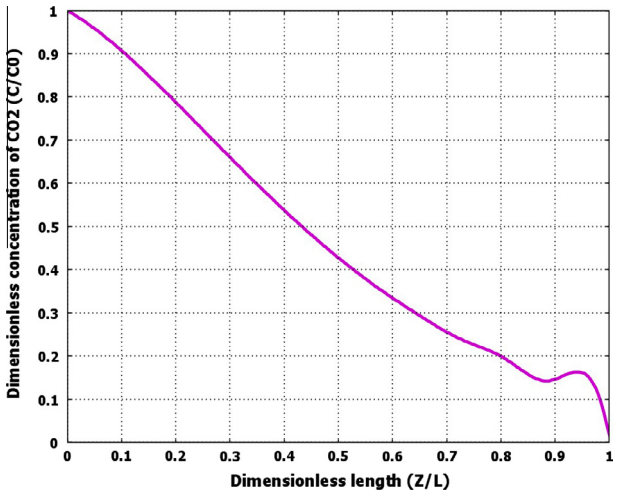

Figure 7 The profile of carbon dioxide concentration in the tube (gas channel) in axial direction (z-direction).

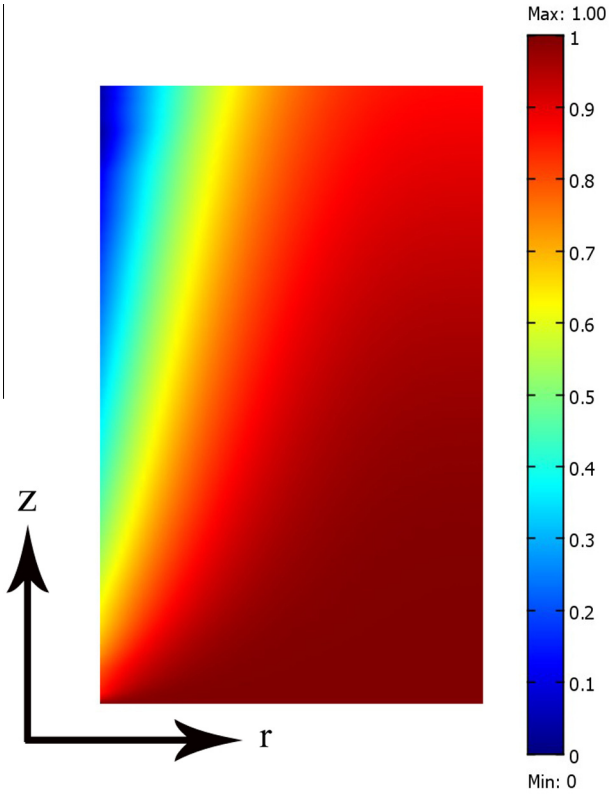

Figure 8 Dimensionless concentration of potassium threonate in the shell of the HFMC.

side. Consequently, absorbent concentration reduces along the HFMC considerably due to consumption of solvent. Axial concentration distribution of potassium threonate along the contactor can be observed in Fig. 9. The absorbent concentration decays in the middle of HFMC length faster than entrance region of HFMC. It is due to the fact that CO_2 concentration in the entrance of shell side is negligible. Therefore, concentration of absorbent solution in the mentioned region

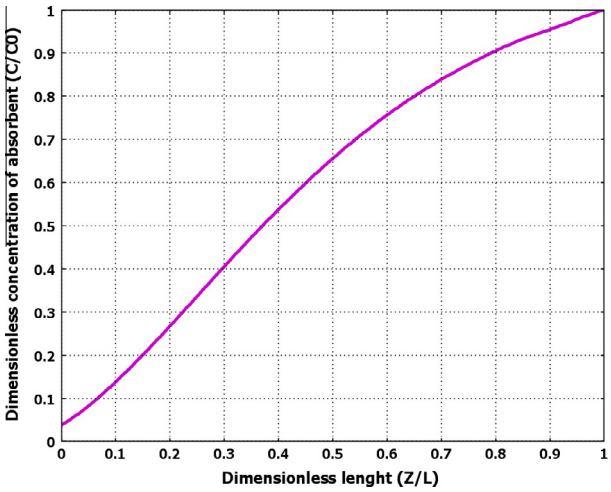

Figure 9 Axial variation of potassium threonate concentration along the HFMC.

has not changed significantly. Fig. 10 indicates total flux of CO_2 and absorbent simultaneously that helps to perceive the mechanism of system functioning.

3.5. Effects of gas and liquid flow rates on CO_2 capture

In this section, simultaneous performance of potassium threonate and DEA absorbents is compared to evaluate the efficiency of separation process using each absorbent. Figs. 11 and 12 show relationship between reaction rate of CO_2 and the two mentioned absorbents versus liquid and gas flow rate, respectively. As it can be seen in Fig. 11, for both

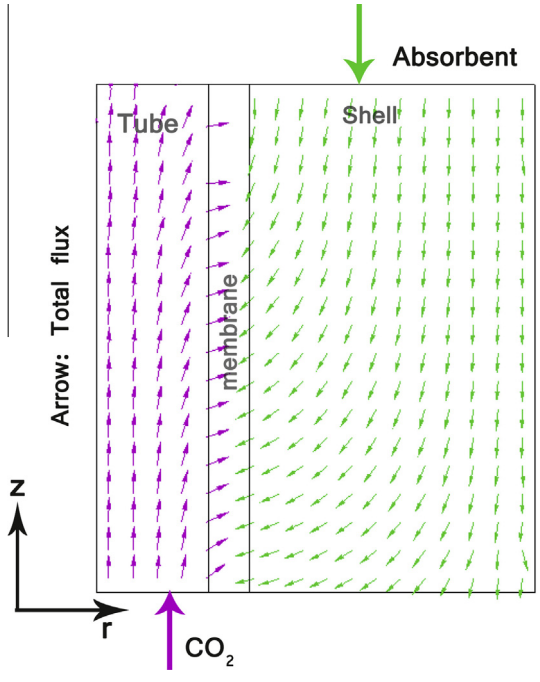

Figure 10 Total flux of CO_2 and absorbent in the membrane module.

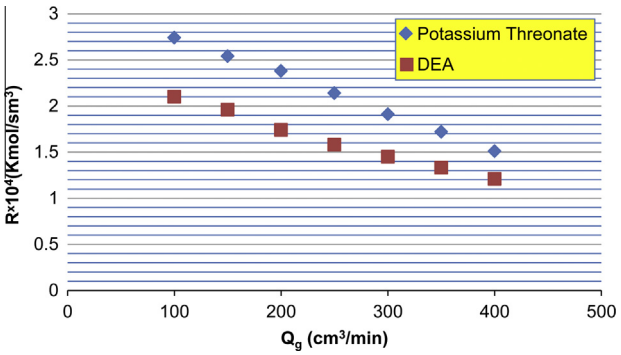

Figure 11 Correlation between reaction rate and gas flow rate.

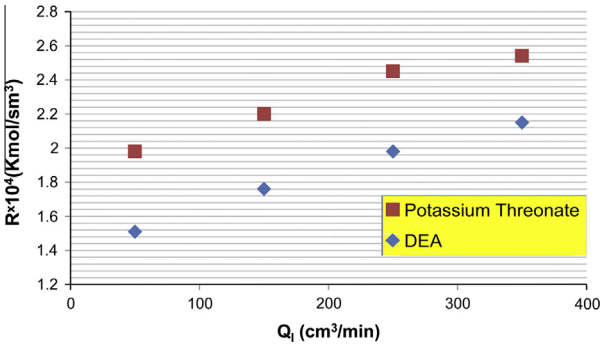

Figure 12 Correlation between reaction rate and liquid flow rate.

absorbents, the reaction rate increases by increase of liquid flow rate. This is because of the fact that the enhancement of liquid flow rate results in increase of Reynolds number and consequently mass transfer coefficient. Additionally, with further increment of liquid flow rate, reaction rate of CO_2 removal does not alter significantly. Therefore, optimum amount of absorbent could be achieved and costs due to expensive absorbents and environmental problems attributed to it, will be decreased. It is obvious from this figure that efficiency of potassium threonate is higher than DEA considerably and for all of the liquid flow rates, reaction rate of potassium threonate is much more than DEA. Therefore it seems that potassium threonate is better absorbent for CO_2 capture than DEA. Fig. 12 shows variation of reaction rate of CO_2 with absorber as a function of gas flow rate. According to this figure, enhancement of gas flow rate results in decrease of reaction rate. This could be due to the fact that as gas flow rate increases, resistance time in the contactor declines. Consequently absorption of CO_2 to liquid phase decreases.

4. Conclusions

In this study, simulation of CO_2 capture by potassium threonate through HFMCs was conducted using CFD technique. Numerical method of finite element was applied to solve equations of mass transfer and a two dimensional mathematical model for prediction of the CO_2 absorption through the HFMC was developed. Because of importance of absorbent

types in gas separation, function of two absorbents of potassium threonate and DEA was compared. Comparison of model predictions with experimental results reveals that reasonable agreement exists between them. Simulation results reveal that potassium threonate can be considered as a more efficient absorber as compared with DEA. According to the model results, that increment of absorbent concentration and flow rate eventuate in increment of CO_2 absorption. On the contrary, enhancement of gas flow rate reduces CO_2 capture. It can be concluded from the obtained results that the proposed model in this work can well predict CO_2 removal through the HFMCs.

References

Adewole, J.K. et al, 2013. Current challenges in membrane separation of CO_2 from natural gas: a review. Int. J. Greenhouse Gas Control 17, 46–65.

Bird, R.B., Stewart, W.E., Lightfoot, E.N., 1960. Transport Phenomena. John Wiley & Sons, New York.

Blauwhoff, P.M.M., Versteeg, G.F., Van Swaaij, W.P.M., 1984. A study on the reaction between CO_2 and alkanolamines in aqueous solutions. Chem. Eng. Sci. 39 (2), 207–225.

Chew, T.-L., Ahmad, A.L., Bhatia, S., 2010. Ordered mesoporous silica (OMS) as an adsorbent and membrane for separation of carbon dioxide (CO_2). Adv. Colloid Interface Sci. 153 (1–2), 43–57.

Fadaei, F., Shirazian, S., Ashrafizadeh, S.N., 2011a. Mass transfer modeling of ion transport through nanoporous media. Desalination 281 (1), 325–333.

Fadaei, F., Shirazian, S., Ashrafizadeh, S.N., 2011b. Mass transfer simulation of solvent extraction in hollow-fiber membrane contactors. Desalination 275 (1–3), 126–132.

Fadaei, F. et al, 2012. Mass transfer simulation of ion separation by nanofiltration considering electrical and dielectrical effects. Desalination 284, 316–323.

Fasihi, M. et al, 2012. Computational fluid dynamics simulation of transport phenomena in ceramic membranes for SO_2 separation. Math. Comput. Modell. 56 (11–12), 278–286.

Fazaeli, R. et al, 2015. Computational simulation of CO_2 removal from gas mixture by chemical absorbent in porous membrane. RSC Adv. 5, 36787. http://dx.doi.org/10.1039/C5RA02001H.

Ghadiri, M., Ashrafizadeh, S.N., 2014. Mass transfer in molybdenum extraction from aqueous solutions using nanoporous membranes. Chem. Eng. Technol. 37 (4), 597–604.

Ghadiri, M., Shirazian, S., 2013. Computational simulation of mass transfer in extraction of alkali metals by means of nanoporous membrane extractors. Chem. Eng. Process. 69, 57–62.

Ghadiri, M. et al, 2013a. Computational simulation for transport of priority organic pollutants through nanoporous membranes. Chem. Eng. Technol. 36 (3), 507–512.

Ghadiri, M., Fakhri, S., Shirazian, S., 2013b. Modeling and CFD simulation of water desalination using nanoporous membrane contactors. Ind. Eng. Chem. Res. 52 (9), 3490–3498.

Ghadiri, M., Marjani, A., Shirazian, S., 2013c. Mathematical modeling and simulation of CO_2 stripping from monoethanolamine solution using nano porous membrane contactors. Int. J. Greenhouse Gas Control 13, 1–8.

Ghadiri, M. et al, 2014a. Simulation of membrane distillation for purifying water containing 1,1,1-trichloroethane. Chem. Eng. Technol. 37 (3), 543–550.

Ghadiri, M., Fakhri, S., Shirazian, S., 2014b. Modeling of water transport through nanopores of membranes in direct-contact membrane distillation process. Polym. Eng. Sci. 54 (3), 660–666.

Ghadiri, M., Asadollahzadeh, M., Hemmati, A., 2015. CFD simulation for separation of ion from wastewater in a membrane contactor. J. Water Process Eng. 6, 144–150.

Han, S.H., Lee, Y.M., 2011. Chapter 4 recent high performance polymer membranes for CO_2 separation. In: Membrane Engineering for the Treatment of Gases: Volume 1: Gas-Separation Problems with Membranes. The Royal Society of Chemistry, pp. 84–124.

Happel, J., 1959. Viscous flow relative to arrays of cylinders. AIChE J. 5 (2), 174–177.

Hemmati, M. et al, 2015. Phenol removal from wastewater by means of nanoporous membrane contactors. J. Ind. Eng. Chem. 21, 1410–1416.

Hoshyargar, V. et al, 2012. Prediction of flow behavior of crude oil-in-water emulsion through the pipe by using rheological properties. Orient. J. Chem. 28 (1), 109–113.

Khansary, M.A., Sani, A.H., Shirazian, S., 2015. Mathematical-thermodynamic solubility model developed by the application of discrete Volterra functional series theory. Fluid Phase Equilib. 385, 205–211.

Kohnehshahri, R.K. et al, 2011. Modeling and numerical simulation of catalytic reforming reactors. Orient. J. Chem. 27 (4), 1351–1355.

Li, J.-L., Chen, B.-H., 2005. Review of CO_2 absorption using chemical solvents in hollow fiber membrane contactors. Sep. Purif. Technol. 41 (2), 109–122.

Lin, S.-H. et al, 2008. Absorption of carbon dioxide by the absorbent composed of piperazine and 2-amino-2-methyl-1-propanol in PVDF membrane contactor. J. Chin. Inst. Chem. Eng. 39 (1), 13–21.

Lu, J.-G. et al, 2007. Effects of activators on mass-transfer enhancement in a hollow fiber contactor using activated alkanolamine solutions. J. Membr. Sci. 289 (1–2), 138–149.

Mandal, B.P., Bandyopadhyay, S.S., 2005. Simultaneous absorption of carbon dioxide and hydrogen sulfide into aqueous blends of 2-amino-2-methyl-1-propanol and diethanolamine. Chem. Eng. Sci. 60 (22), 6438–6451.

Marjani, A., Shirazian, S., 2010. CFD simulation of dense gas extraction through polymeric membranes. World Acad. Sci., Eng. Technol. 37, 1043–1047.

Marjani, A., Shirazian, S., 2011a. Simulation of heavy metal extraction in membrane contactors using computational fluid dynamics. Desalination 281 (1), 422–428.

Marjani, A., Shirazian, S., 2011b. Hydrodynamic investigations on heavy metal extraction in membrane extractors. Orient. J. Chem. 27 (4), 1311–1316.

Marjani, A., Shirazian, S., 2011c. Computational fluid dynamics simulation of ammonia removal from wastewaters by membrane. Asian J. Chem. 23 (7), 3299–3300.

Marjani, A., Shirazian, S., 2011d. Investigation on copper extraction using numerical simulation. Asian J. Chem. 23 (7), 3289–3290.

Marjani, A., Shirazian, S., 2011e. Investigation on numerical simulation of acetone and ethanol separation from water by using membrane. Asian J. Chem. 23 (7), 3293–3294.

Marjani, A., Shirazian, S., 2012a. CFD simulation of mass transfer in membrane evaporators for concentration of aqueous solutions. Orient. J. Chem. 28 (1), 83–87.

Marjani, A., Shirazian, S., 2012b. Modeling of organic mixtures separation in dense membranes using finite element method (FEM). Orient. J. Chem. 28 (1), 41–46.

Marjani, A., Shirazian, S., 2012c. Theoretical studies on copper extraction by means of polymeric membrane contactors. Orient. J. Chem. 28 (1), 23–28.

Marjani, A., Shirazian, S., 2012d. Application of CFD techniques for prediction of NH_3 transport through porous membranes. Orient. J. Chem. 28 (1), 67–72.

Marjani, A., Shirazian, S., 2012e. Mathematical modeling and CFD simulation of hydrocarbon purification using membrane technology. Orient. J. Chem. 28 (1), 123–129.

Marjani, A., Rezakazemi, M., Shirazian, S., 2011a. Vapor pressure prediction using group contribution method. Orient. J. Chem. 27 (4), 1331–1335.

Marjani, A., Shirazi, Y., Shirazian, S., 2011b. Investigation on the best conditions for purification of multiwall carbon nanotubes. Asian J. Chem. 23 (7), 3205–3207.
Marjani, A., Mohammadi, P., Shirazian, S., 2012a. Preparation and characterization of poly (vinyl alcohol) membrane for pervaporation separation of water–organic mixtures. Orient. J. Chem. 28 (1), 97–102.
Marjani, A., Rezakazemi, M., Shirazian, S., 2012b. Simulation of methanol production process and determination of optimum conditions. Orient. J. Chem. 28 (1), 145–151.
Marjani, A. et al, 2012c. Mathematical modeling of gas separation in flat-sheet membrane contactors. Orient. J. Chem. 28 (1), 13–18.
Miramini, S.A., Razavi, S.M.R., Ghadiri, M., Mahdavi, S.Z., Moradi, S., 2013. CFD simulation of acetone separation from an aqueous solution using supercritical fluid in a hollow-fiber membrane contactor. Chem. Eng. Process: Process Intensif. 72, 130–136. http://dx.doi.org/10.1016/j.cep.2013.07.005.
Moghadassi, A. et al, 2011. Gas separation properties of hollow-fiber membranes of polypropylene and polycarbonate by melt-spinning method. Asian J. Chem. 23 (5), 1922–1924.
Mohammadi, M. et al, 2015. Separation of greenhouse gases from gas mixtures using nanoporous polymeric membranes. Polym. Eng. Sci. 55 (5), 975–980.
Moradi, S. et al, 2013. 3 Dimensional hydrodynamic analysis of concentric draft tube airlift reactors with different tube diameters. Math. Comput. Modell. 57 (5–6), 1184–1189.
Nosratinia, F., Ghahremani, H., Shirazian, S., 2015. Preparation and characterization of nanoporous ceramic membranes for separation of water from ethanol. Desalination Water Treat. 54 (6), 1550–1555.
Pishnamazi, M. et al, 2012. Mathematical modeling and numerical simulation of wastewater treatment unit using CFD. Orient. J. Chem. 28 (1), 51–58.
Portugal, A.F., Magalhães, F.D., Mendes, A., 2008. Carbon dioxide absorption kinetics in potassium threonate. Chem. Eng. Sci. 63 (13), 3493–3503.
Ranjbar, M. et al, 2013. Computational fluid dynamics simulation of mass transfer in the separation of fermentation products using nanoporous membranes. Chem. Eng. Technol. 36 (5), 728–732.
Razavi, S.M.R. et al, 2013. CFD simulation of CO_2 capture from gas mixtures in nanoporous membranes by solution of 2-amino-2-methyl-1-propanol and piperazine. Int. J. Greenhouse Gas Control 15, 142–149.
Razavi, S.M.R., Marjani, A., Shirazian, S., 2014. CO_2 capture from gas mixtures by alkanol amine solutions in porous membranes. Transp. Porous Media 106 (2), 323–338.
Razavi, S.M.R., Shirazian, S., Najafabadi, M.S., 2015. Investigations on the ability of Di-isopropanol amine solution for removal of CO_2 from natural gas in porous polymeric membranes. Polym. Eng. Sci. 55 (3), 598–603.
Ren, J. et al, 2006. Effect of PVDF dope rheology on the structure of hollow fiber membranes used for CO_2 capture. J. Membr. Sci. 281 (1–2), 334–344.
Rezakazemi, M. et al, 2011a. CFD simulation of natural gas sweetening in a gas–liquid hollow-fiber membrane contactor. Chem. Eng. J. 168 (3), 1217–1226.
Rezakazemi, M. et al, 2011b. CFD simulation of water removal from water/ethylene glycol mixtures by pervaporation. Chem. Eng. J. 168 (1), 60–67.
Rezakazemi, M., Shirazian, S., Ashrafizadeh, S.N., 2012. Simulation of ammonia removal from industrial wastewater streams by means of a hollow-fiber membrane contactor. Desalination 285, 383–392.
Rezakazemi, M. et al, 2013a. Numerical modeling and optimization of wastewater treatment using porous polymeric membranes. Polym. Eng. Sci. 53 (6), 1272–1278.
Rezakazemi, M. et al, 2013b. Transient computational fluid dynamics modeling of pervaporation separation of aromatic/aliphatic hydrocarbon mixtures using polymer composite membrane. Polym. Eng. Sci. 53 (7), 1494–1501.
Rezakazemi, M., Marjani, A., Shirazian, S., 2013c. Development of a group contribution method based on UNIFAC groups for the estimation of vapor pressures of pure hydrocarbon compounds. Chem. Eng. Technol. 36 (3), 483–491.
Shirazian, S., Ashrafizadeh, S.N., 2010a. Mass transfer simulation of caffeine extraction by subcritical CO_2 in a hollow-fiber membrane contactor. Solvent Extr. Ion Exch. 28 (2), 267–286.
Shirazian, S., Ashrafizadeh, S.N., 2010b. Mass transfer simulation of carbon dioxide absorption in a hollow-fiber membrane contactor. Sep. Sci. Technol. 45 (4), 515–524.
Shirazian, S., Ashrafizadeh, S.N., 2011. Near-critical extraction of the fermentation products by membrane contactors: a mass transfer simulation. Ind. Eng. Chem. Res. 50 (4), 2245–2253.
Shirazian, S., Ashrafizadeh, S.N., 2013. 3D modeling and simulation of mass transfer in vapor transport through porous membranes. Chem. Eng. Technol. 36 (1), 177–185.
Shirazian, S., Ashrafizadeh, S.N., 2014. Optimum conditions for the synthesis of CHA-type zeolite membranes applicable to the purification of natural gas. Ind. Eng. Chem. Res. 53 (31), 12435–12444.
Shirazian, S., Ashrafizadeh, S.N., 2015a. Synthesis of substrate-modified LTA zeolite membranes for dehydration of natural gas. Fuel 148, 112–119.
Shirazian, S., Ashrafizadeh, S.N., 2015b. Investigations on permeation of water vapor through synthesized nanoporous zeolite membranes. A mass transfer model. RSC Adv. 5 (39), 30719–30726.
Shirazian, S., Ashrafizadeh, S.N., 2015c. LTA and ion-exchanged LTA zeolite membranes for dehydration of natural gas. J. Ind. Eng. Chem. 22, 132–137.
Shirazian, S., Moghadassi, A., Moradi, S., 2009. Numerical simulation of mass transfer in gas–liquid hollow fiber membrane contactors for laminar flow conditions. Simul. Model. Pract. Theory 17 (4), 708–718.
Shirazian, S., Marjani, A., Fadaei, F., 2011a. Supercritical extraction of organic solutes from aqueous solutions by means of membrane contactors: CFD simulation. Desalination 277 (1–3), 135–140.
Shirazian, S., Marjanm, A., Azizmohammadi, F., 2011b. Prediction of SO_2 transport across ceramic membranes using finite element method (FEM). Orient. J. Chem. 27 (2), 485–490.
Shirazian, S., Marjani, A., Rezakazemi, M., 2012a. Separation of CO_2 by single and mixed aqueous amine solvents in membrane contactors: fluid flow and mass transfer modeling. Eng. Comput. 28 (2), 189–198.
Shirazian, S. et al, 2012b. Development of a mass transfer model for simulation of sulfur dioxide removal in ceramic membrane contactors. Asia-Pac. J. Chem. Eng. 7 (6), 828–834.
Shirazian, S., Fadaei, F., Ashrafizadeh, S.N., 2012c. Modeling of thallium extraction in a hollow-fiber membrane contactor. Solvent Extr. Ion Exch. 30 (5), 490–506.
Shirazian, S. et al, 2012d. Implementation of the finite element method for simulation of mass transfer in membrane contactors. Chem. Eng. Technol. 35 (6), 1077–1084.
Shirazian, S. et al, 2012e. Hydrodynamics and mass transfer simulation of wastewater treatment in membrane reactors. Desalination 286, 290–295.
Shirazian, S., Parto, S.G., Ashrafizadeh, S.N., 2014. Effect of water content of synthetic hydrogel on dehydration performance of nanoporous LTA zeolite membranes. Int. J. Appl. Ceram. Technol. 11 (5), 793–803.
Sohrabi, M.R. et al, 2011a. Theoretical studies on membrane-based gas separation using computational fluid dynamics (CFD) of mass transfer. J. Chem. Soc. Pak. 33 (4), 464–473.
Sohrabi, M.R. et al, 2011b. Preparation and simulation of polycarbonate hollow-fiber membrane for gas separation. Asian J. Chem. 23 (1), 302–304.

Sohrabi, M.R. et al, 2011c. Mathematical modeling and numerical simulation of CO_2 transport through hollow-fiber membranes. Appl. Math. Model. 35 (1), 174–188.

Sohrabi, M.R. et al, 2011d. Simulation studies on H_2S absorption in potassium carbonate aqueous solution using a membrane module. Asian J. Chem. 23 (9), 4227–4228.

Sohrabi, M.R. et al, 2011e. Simulation of ethanol and acetone extraction from aqueous solutions in membrane contactors. Asian J. Chem. 23 (9), 4229–4230.

Spillman, R., 1995. Chapter 13 economics of gas separation membrane processes. In: Richard, D.N., Stern, S.A. (Eds.), Membrane Science and Technology. Elsevier, pp. 589–667.

Tahvildari, K., Razavi, S.M.R., Tavakoli, H., Mashayekhi, A., Golmohammadzadeh, R., 2016. Modeling and simulation of membrane separation process using computational fluid dynamics. Arabian J. Chem. 9 (1), 72–78.

Thiruvenkatachari, R. et al, 2009. Post combustion CO_2 capture by carbon fibre monolithic adsorbents. Prog. Energy Combust. Sci. 35 (5), 438–455.

Valavi, M. et al, 2013. Calculation of the density and activity of water in ATPS systems for separation of biomolecules. J. Solut. Chem. 42 (7), 1423–1437.

Yeo, Z.Y. et al, 2012. Conventional processes and membrane technology for carbon dioxide removal from natural gas: a review. J. Nat. Gas Chem. 21 (3), 282–298.

Zhang, Y. et al, 2013. Current status and development of membranes for CO_2/CH_4 separation: a review. Int. J. Greenhouse Gas Control 12, 84–107.